

PAPER

Triggered-release polymeric conjugate micelles for on-demand intracellular drug delivery

To cite this article: Yanwu Cao *et al* 2015 *Nanotechnology* **26** 115101

View the [article online](#) for updates and enhancements.

Related content

- [Covalent and non-covalent curcumin loading in acid-responsive polymeric micellar nanocarriers](#)

Min Gao, Chao Chen, Aiping Fan *et al.*

- [One-pot synthesis of crosslinked amphiphilic polycarbonates as stable but reduction-sensitive carriers for doxorubicin delivery](#)

Xiaoqing Yi, Quan Zhang, Hui Dong *et al.*

- [pH-responsive polymer-drug conjugates as multifunctional micelles for cancer-drug delivery](#)

Yang Kang, Wei Ha, Ying-Qian Liu *et al.*

Recent citations

- [pH-sensitive curcumin conjugated micelles for tumor triggered drug delivery](#)

Hamid Rashidzadeh *et al*

- [GSH responsive nanomedicines self-assembled from small molecule prodrug alleviate the toxicity of cardiac glycosides as potent cancer drugs](#)

Huiyun Zhang *et al*

- [Disulfide-Mediated Bioconjugation: Disulfide Formation and Restructuring on the Surface of Nanomanufactured \(Microfluidics\) Nanoparticles](#)

Mike Geven *et al*



IOP | ebooks™

Bringing together innovative digital publishing with leading authors from the global scientific community.

Start exploring the collection—download the first chapter of every title for free.

Triggered-release polymeric conjugate micelles for on-demand intracellular drug delivery

Yanwu Cao¹, Min Gao¹, Chao Chen¹, Aiping Fan¹, Ju Zhang², Deling Kong², Zheng Wang¹, Dan Peer^{3,4,5} and Yanjun Zhao¹

¹ School of Pharmaceutical Science & Technology, Tianjin Key Laboratory for Modern Drug Delivery & High Efficiency, and Collaborative Innovation Center of Chemical Science and Engineering, Tianjin University, Tianjin 300072, People's Republic of China

² State Key Laboratory of Medicinal Chemical Biology, Key Laboratory of Bioactive Materials, Ministry of Education, College of Life Science and Collaborative Innovation Center of Chemical Science and Engineering, Nankai University, Tianjin 300071, People's Republic of China

³ Laboratory of Nanomedicine, Department of Cell Research and Immunology, George S. Wise Faculty of Life Sciences, Israel

⁴ Department of Materials Sciences and Engineering, Faculty of Engineering, Israel

⁵ Center for Nanoscience and Nanotechnology, Tel Aviv University, Tel Aviv 69978, Israel

E-mail: zhaoyj@tju.edu.cn

Received 11 December 2014, revised 23 January 2015

Accepted for publication 27 January 2015

Published 24 February 2015

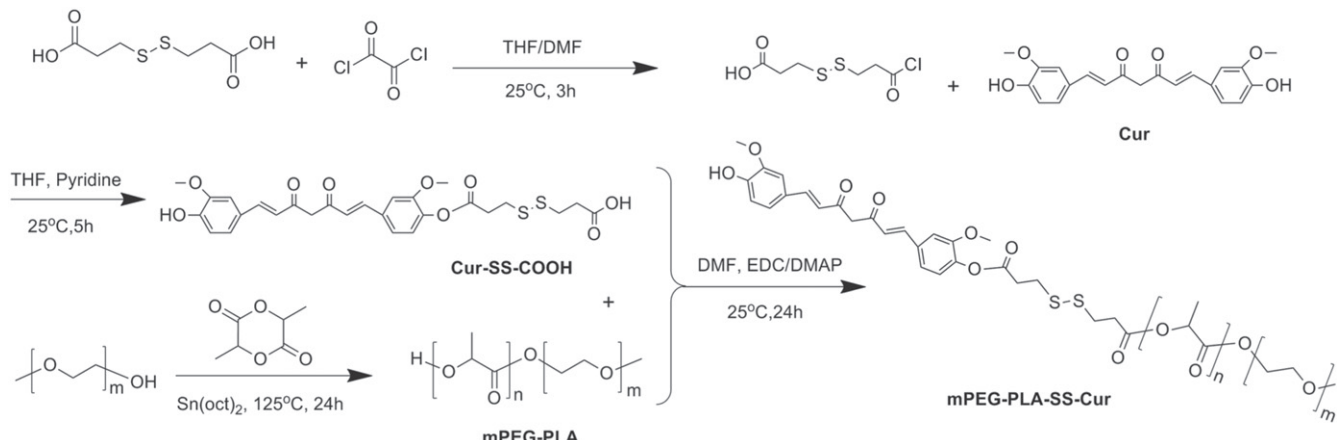


Abstract

Nanoscale drug delivery platforms have been developed over the past four decades that have shown promising clinical results in several types of cancer and inflammatory disorders. These nanocarriers carrying therapeutic payloads are maximizing the therapeutic outcomes while minimizing adverse effects. Yet one of the major challenges facing drug developers is the dilemma of premature versus on-demand drug release, which influences the therapeutic regimen, efficacy and potential toxicity. Herein, we report on redox-sensitive polymer-drug conjugate micelles for on-demand intracellular delivery of a model active agent, curcumin. Biodegradable methoxy poly(ethylene glycol)-poly(lactic acid) copolymer (mPEG-PLA) was conjugated with curcumin via a disulfide bond or ester bond (control), respectively. The self-assembled redox-sensitive micelles exhibited a hydrodynamic size of 115.6 ± 5.9 nm with a zeta potential of -10.6 ± 0.7 mV. The critical micelle concentration was determined at 6.7 ± 0.4 $\mu\text{g mL}^{-1}$. Under sink conditions with a mimicked redox environment (10 mM dithiothreitol), the extent of curcumin release at 48 h from disulfide bond-linked micelles was nearly three times higher compared to the control micelles. Such rapid release led to a lower half maximal inhibitory concentration (IC_{50}) in HeLa cells at 18.5 ± 1.4 $\mu\text{g mL}^{-1}$, whereas the IC_{50} of control micelles was 41.0 ± 2.4 $\mu\text{g mL}^{-1}$. The cellular uptake study also revealed higher fluorescence intensity for redox-sensitive micelles. In conclusion, the redox-sensitive polymeric conjugate micelles could enhance curcumin delivery while avoiding premature release, and achieving on-demand release under the high glutathione concentration in the cell cytoplasm. This strategy opens new avenues for on-demand drug release of nanoscale intracellular delivery platforms that ultimately might be translated into pre-clinical and future clinical practice.

Keywords: polymeric conjugate, micelle, curcumin, redox-sensitive, on-demand delivery, triggered-release

(Some figures may appear in colour only in the online journal)



Scheme 1. Synthetic route of curcumin derivative Cur-SS-COOH and redox-responsive polymer-curcumin conjugate mPEG-PLA-SS-Cur. mPEG, PLA, SS, and Cur represents poly(ethylene glycol), poly(lactic acid), disulfide bond, and curcumin, respectively.

1. Introduction

Nanoscale particulate anti-tumor drug delivery systems have been extensively studied over the past few decades, and have shown promising features such as superior capability to deliver therapeutic payloads, reduce adverse effects, and improve therapeutic efficacy [1–3]. In addition, nanoparticle-based strategies improve solubilization of hydrophobic drugs and extend blood circulation, which could benefit passive tumor tissue targeting and active cellular targeting; they have also been effective in combinational co-delivery of multiple active agents, active in reversing cancer multidrug resistance, and capable of combining imaging with therapeutics (i.e. theranostic systems) [4–12]. In spite of these distinct advantages, one of the dilemmas that needs to be addressed in drug delivery systems for therapeutic intervention in cancer is the issue of premature versus on-demand drug release [13].

Premature drug release is a phenomenon wherein a significant amount of active agent is released during systemic circulation prior to reaching the target site, since the human blood maintains a perfect sink condition. This is particularly manifest for the situation where the drug was physically (non-covalently) associated with the nanoparticles and both exhibited poor affinity to a potential target site. On-demand drug release could be ideal for therapeutics since the drug is secured in nanoparticles and not liberated until getting to the target site. Avoiding premature release necessitates the entrapment of drug within nanoparticles, or the covalent attachment of a given drug to a nanoparticle. However, such strategies could also introduce other hurdles such as poor drug release, which would result in low intracellular drug concentration, and thus delay the onset of the pharmacological action [14, 15].

Tailored design of stimuli-responsive nanoparticles offers an efficient solution to address the challenge of premature versus on-demand drug release [16]. The advances of material science and nanoparticle fabrication technology make such smart design possible via the utilization of various triggers, e.g. ultrasound, temperature, magnetic field, light, enzyme, pH, and redox potential [17]. Among these, the employment

of redox potential to initiate on-demand drug release shows great promise to address the challenge mentioned above, because the glutathione (GSH) concentration in the cytoplasm (mM) is almost three orders higher compared to that in the systemic circulation (μM) [18]. Although many redox-responsive nanoparticles have been previously reported, to the best of our knowledge, their role in addressing premature drug release has not been investigated.

The aim of this study was to generate and assess polymer-drug conjugate micellar nanoparticles *in vitro* to realize redox-triggered intracellular drug delivery without premature dose reduction. Amphiphilic polymer-drug conjugate is used simply because premature drug release is presumed to be absent due to the covalent linking between the drug and the polymer, and in addition, the conjugate can self-assemble into nanoparticles in aqueous media [15]. A pleiotropic anticancer compound, curcumin, was selected as the active agent. Biodegradable methoxy poly(ethylene glycol)-poly(lactic acid) (mPEG-PLA) copolymer was utilized as the amphiphilic polymer that was connected to the model drug via a disulphide bond.

2. Experimental

2.1. Materials

Curcumin, ethanol, dimethylformamide (DMF), dichloromethane (DCM), 1,2-dichloroethane, pyridine, anhydrous sodium sulphate, citric acid, disodium hydrogen phosphate, sodium hydroxide, and sodium dodecyl sulphate (SDS) were purchased from the Institute of Guangfu Fine Chemical Research (Tianjin, China). Methanol and tetrahydrofuran (THF) were obtained from Concord (Tianjin, China). Oxalyl chloride and 3,3'-dithiodipropionic acid were from Sahn Chemicals (Shanghai, China). Pyrene, 4-dimethylaminopyridine, N,N'-dicyclohexylcarbodiimide (DCC), stannous octoate, 4-dimethylaminopyridine (DMAP) and glutaric anhydride were sourced from Jingchun Reagents (Shanghai, China). N-(3-Dimethylaminopropyl)-N'-ethylcarbodiimide

hydrochloride (EDC-HCl) was from Medpep Co., Ltd (Shanghai, China). Methoxy poly(ethylene glycol) (mPEG, 2000 Da) and 4',6-diamidino-2-phenylindole (DAPI) were obtained from Sigma-Aldrich (Beijing, China). D,L-lactide was from Daigang Biomaterial Co., Ltd (Jinan, China). The human epithelial carcinoma (HeLa) cell line was provided by the Institute of Biomedical Engineering (Chinese Academy of Medical Sciences & Peking Union Medical College). Dulbecco's modification of eagle's medium (DMEM), fetal bovine serum, and penicillin-streptomycin were from HyClone Inc. (Logan City, Utah, USA). Cell Counting Kit-8 (CCK-8) was from Dojindo Laboratories (Shanghai, China). All other chemicals were sourced from Jiangtian Chemicals (Tianjin, China).

2.2. Synthesis of curcumin derivatives

Mono-carboxyl-terminated curcumin (Cur-COOH) was synthesized based on a previously published method [15]. Disulfide bond-containing mono-carboxyl-terminated curcumin (Cur-SS-COOH) was generated as detailed (scheme 1). 3,3'-dithiodipropionic acid (0.2103 g, 1 mmol) and 40 μ L DMF were mixed in 10 mL anhydrous THF maintained at 0 °C. Oxalyl chloride (105 μ L, 1.2 mmol) was then dropwise added to the above solution. The mixture was kept at ambient temperature (25 °C) for 3 h ready for further use. Curcumin (0.3684 g, 1 mmol) and pyridine (806 μ L, 10 mmol) were co-dissolved in 10 mL THF, which was followed by the slow supplementation of the above solution with light protection. After 5 h, THF was removed and the residue was dissolved in 30 mL DCM. The obtained solution was washed by a 30 mL hydrochloride solution (0.1 mM) in triplicate. The organic phase was then collected, followed by DCM removal. The attained crude product was dissolved in 4 mL DCM and purified by silica gel column chromatography, eluted by a mixture of DCM and methanol (100:1, v/v) containing 1% (v/v) acetic acid. The final product Cur-SS-COOH was collected (yield: 58.4%). 1 H NMR (600 MHz, CDCl₃), δ [ppm]: 7.55-7.47 (m, 2H), 7.10-6.82 (m, 6H), 6.43 (m, 2H), 5.74 (s, 1H), 3.85 (s, 3H), 3.78 (s, 3H), 3.00-2.93 (m, 4H), 2.89 (t, 2H), 2.74 (t, 2H).

2.3. Synthesis of polymeric conjugate

The generation of amphiphilic mPEG-PLA copolymer and ester bond-linked polymer-curcumin conjugate (i.e. mPEG-PLA-Cur) employed a previously published method [15]. Disulfide-containing polymeric conjugate (i.e. mPEG-PLA-SS-Cur) was produced as follows (scheme 1). Cur-SS-COOH (0.1268 g, 0.2264 mmol), mPEG-PLA (0.8895 g, 0.2516 mmol), EDC-HCl (0.0434 g, 0.2264 mmol), and DMAP (0.0277 g, 0.2264 mmol) were co-dissolved in 10 mL DMF and the reaction was maintained at ambient temperature under the nitrogen atmosphere with light protection. After 24 h, the crude product was purified by repeated precipitation in ice-cold diethyl ether, filtration and vacuum-drying to get the purified mPEG-PLA-SS-Cur (yield: 72.3%). 1 H NMR (600 MHz, CDCl₃), δ [ppm]: 7.59 (m, 2H), 7.21-6.81

(m, 6H), 6.56 (m, 2H), 5.86 (s, 1H), 5.17 (s, -CH PLA repeating unit), 3.90-3.74 (m, 6H), 3.65 (m, -CH₂ PEG repeating unit), 3.38 (s, -CH₃ PEG end group), 3.13-2.97 (m, 8H), 1.57 (s, -CH₃ PLA repeating unit).

2.4. Molecular weight determination

The molecular weight and molecular weight distribution of both mPEG-PLA-Cur and mPEG-PLA-SS-Cur conjugates were determined by gel permeation chromatography (Malvern Viscotek TDA 305). THF was used as the eluent as well as the solvent to dissolve both samples at a concentration of 5 mg mL⁻¹. The elution rate was 1 mL min⁻¹ at 25 °C with polystyrene as the calibration standard.

2.5. Micelle preparation

The polymeric conjugate micelles were prepared by a typical dialysis method [15]. In brief, mPEG-PLA-Cur or mPEG-PLA-SS-Cur solution in THF (0.1 g mL⁻¹, 10 mL) was sealed in a dialysis bag with a molecular weight cut-off (MWCO) of 2000 Da. The solution was dialyzed against cold water (4 °C, pH 7.0) with light protection. After 24 h, the solution inside the dialysis bag was purified by passing through a 0.45 μ m filter, followed by freeze-drying until ready for use.

2.6. Particle size and zeta potential analysis

The hydrodynamic size and zeta potential of both types of conjugate micelles were determined in phosphate buffer at pH 7.4 (1 mg mL⁻¹) using a Malvern Zetasizer Nano ZS instrument. The measurements were performed at 25 °C in triplicate. The micelle size and morphology was also analyzed by transmission electron microscope (TEM) (JEOL, JEM-100 CXII). The sample solution (1 mg mL⁻¹, 20 μ L) was placed onto collodion-coated copper grids and air-dried prior to image acquisition.

2.7. Micelle stability evaluation

The evaluation of conjugate micelle stability utilized the critical micelle concentration (CMC) as an index. The determination of CMC was based on a typical luminescence spectroscopy approach with pyrene as the probe [15]. In detail, a fixed amount of pyrene (0.5 μ M) was added to the aqueous solution of both types of conjugate micelles with the concentration ranging from 0.4 to 400 (μ g mL⁻¹). After a 12 h incubation, the emission spectra of micelles was documented (350–450 nm) and the excitation wavelength was set at 333 nm with a spectral slit width of 5 nm. A Fluorolog®3-21 spectrofluorometer (HORIBA JobinYvon) was used for the analysis, which was carried out in triplicate. The ratio of sample band intensity at 384 nm and 373 nm was drawn against the logarithm of the micelles' concentration and the flexion point of the curve gave the CMC value.

2.8. Drug release study

The curcumin loading in conjugate micelles was calculated based on the ^1H NMR analysis. The determination of both the drug and copolymer content utilized the methoxyl group of PEG as the reference. The *in vitro* drug release experiments were carried out in the static vertical Franz-type diffusion cells (ca. 17 mL) at 37 °C. The donor phase and receiver fluid were separated by a cellulose membrane (MWCO: 2000 Da). The receiver fluid was phosphate buffer (pH 7.4) containing 5% (w/v) SDS to maintain the sink conditions. Dithiothreitol (DTT) (10 mM) was also present in the receiver fluid to mimic the redox environment in the cytoplasm. The donor phase was filled up with micellar solutions. At pre-determined time points (0.5–48 h), the ca. 0.5 mL receiver fluid was withdrawn from the sampling arm and the same volume of fresh fluid was supplemented. The drug content was analyzed by high performance liquid chromatography (HPLC) coupled with a UV detector based on a previously published method. For the mPEG-PLA-Cur micelles, the released drug was parent curcumin and the UV wavelength was 419 nm. However, the released compound from mPEG-PLA-SS-Cur micelles was the thiol-ended curcumin derivative, Cur-SH, whose detection wavelength was set at 417 nm. The cumulative released drug was plotted against the time needed to get the release profile. A mass balance study at the end of experiment (48 h) was also performed to obtain the total drug recovery ($n=3$).

2.9. Cell viability assay

HeLa cells were maintained in DMEM medium containing 10% fetal bovine serum and 100 kU L $^{-1}$ penicillin-streptomycin in an atmosphere of 5% CO₂ at 37 °C. The cells were seeded in 96-well multiplates at a density of 5×10^3 per well. After a 24 h incubation period, the cells were exposed to three samples (mPEG-PLA-SS-Cur, mPEG-PLA-Cur, and free curcumin) at different concentrations (5–100 µg mL $^{-1}$) for 24 h, respectively. Both micelle samples were transferred by the culture medium, whereas free curcumin was dissolved in PEG 400. Then the CCK-8 reagent was added which was followed by another 30 min incubation period; the cell viability was measured by the absorbance of formazan dye at 459 nm ($n=6$). The IC₅₀ was calculated using the Origin software package (OriginLab, Northampton, MA, USA).

2.10. Cellular uptake

Free curcumin was solubilized in PEG 400 at a concentration of 100 µg mL $^{-1}$; both micelle samples were dispersed in the DMEM medium with an equivalent drug concentration to the free curcumin control. HeLa cells are seeded in the 35-mm cell culture plates at a density of 1×10^4 cells/well in 1 mL culturing medium at the conditions of 5% CO₂ and 37 °C. After 24 h adherent culture, the medium was removed and the cells were washed with PBS (0.5 mL) twice, followed by the supplement of fresh medium (200 µL) and sample solution (200 µL). After a predetermined time course (2 h, 6 h, or 12 h), the curcumin-containing medium was discarded. The

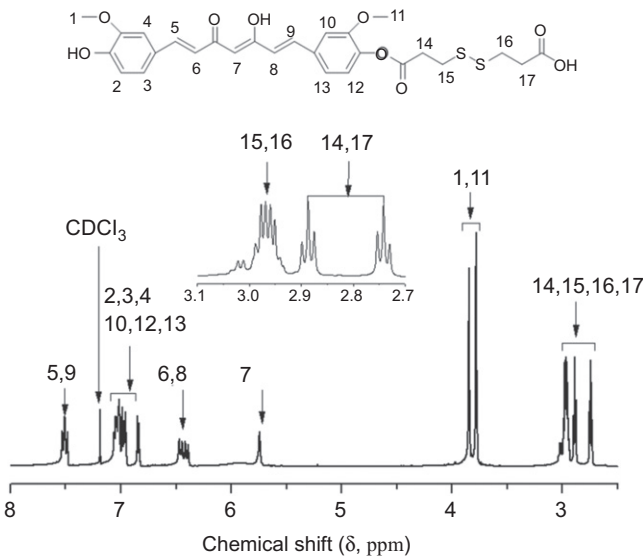


Figure 1. ^1H NMR spectrum of curcumin derivative (Cur-SS-COOH) in CDCl₃. SS and Cur represents disulfide bond, and curcumin, respectively.

cells were washed with PBS (1 mL) in triplicate, and then fixed with paraformaldehyde for 20 min, followed by the PBS washing and nuclear staining with DAPI (20 µL, 1 µg mL $^{-1}$) for 15 min. Then the cells were washed again with PBS, supplemented with 1 mL fresh DMEM medium, and imaged by confocal laser scanning microscope (CLSM) (LSM 710, Zeiss, Germany).

2.11. Statistical analysis

Data were presented as mean \pm standard deviation (SD), and analyzed using a t-test. A statistically significant difference was considered if a p -value was found less than 0.05.

3. Results and discussion

To successfully generate redox-labile polymeric conjugate micelles, it is mandatory to introduce a disulfide bond between the drug and the polymer. In the current study, a linker molecule, 3,3'-dithiodipropionic acid, was brought in connecting with the phenolic hydroxyl group of curcumin, which led to the formation of disulphide-containing curcumin derivative, Cur-SS-COOH (figure 1). Then the mPEG-PLA copolymer was covalently bond with the derivative via an ester bond that resulted in the target conjugate, mPEG-PLA-SS-Cur (figure 2). The conjugate without disulphide, mPEG-PLA-Cur, was also produced as the control [15]. Essentially, the strategy of combining the linker with the drug prior to coupling it with the polymer is superior to the reverse strategy that modifies the polymer with the linker, and then with the curcumin. This is basically because the polymer is characterized by a non-uniform molecular weight and the purification of polymer-linker out of the parent polymer via precipitation or column elution is often difficult since both exhibit similar physicochemical properties [19]. Nevertheless,

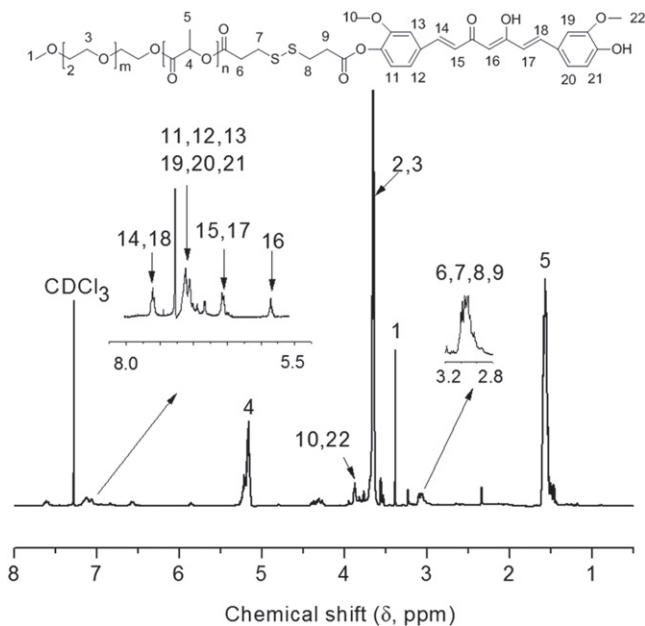


Figure 2. ^1H NMR spectrum of polymer-drug conjugate (mPEG-PLA-SS-Cur) in CDCl_3 . mPEG, PLA, SS, and Cur represents poly(ethylene glycol), poly(lactic acid), disulfide bond, and curcumin, respectively.

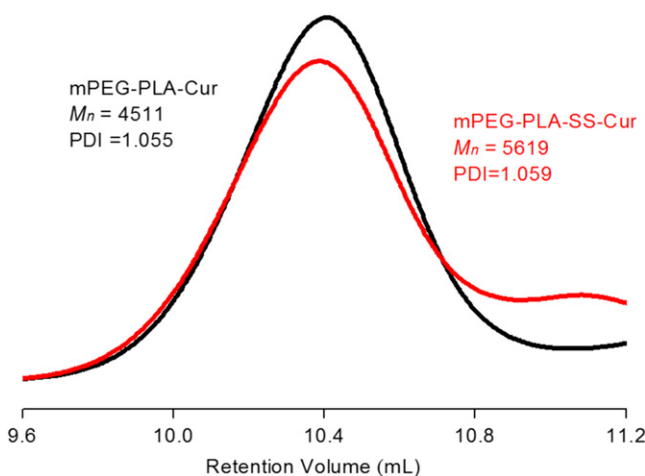


Figure 3. Gel permeation chromatography (GPC) spectra of two types of polymer-drug conjugate (mPEG-PLA-Cur and mPEG-PLA-SS-Cur). The number-averaged molecular weight (M_n) and polydispersity index (PDI) of both conjugates were presented.

the curcumin-linker molecule (i.e. Cur-SS-COOH) is much easier to purify from the parent drug.

With the aid of gel permeation chromatography (GPC), the molecular weight (M_n) of mPEG-PLA-SS-Cur and mPEG-PLA-Cur was determined at 5619 Da and 4511 Da, respectively (figure 3). The polydispersity index (PDI) of both conjugates was below 1.1, which is much lower than the threshold value (1.5) of a broad molecular weight distribution [20]. This indicated that the molecular weights of both polymer-curcumin conjugates were narrowly distributed. The end group analysis via ^1H NMR revealed the molecular weight (M_n) of mPEG-PLA-SS-Cur and mPEG-PLA-Cur was 4231 Da and 4151 Da, respectively. Such discrepancy

between GPC and ^1H NMR determination was a consequence of the strong dependence of conjugate M_n on its architecture as well as the calibrant in terms of GPC analysis. From this point of view, ^1H NMR is valuable, but it cannot give the information of weight-average molecular weight. Therefore, the combination of both techniques would display more reliable molecular weight data of polymer-drug conjugates.

The redox-responsive mPEG-PLA-SS-Cur conjugate as well as the control could capably self-assemble into micellar nanoparticles. The surface charge analysis showed that both samples exhibited a negative zeta potential at $-10.6 \pm 0.7 \text{ mV}$ (mPEG-PLA-SS-Cur) and $-8.2 \pm 0.6 \text{ mV}$ (mPEG-PLA-Cur). The hydrodynamic size of the redox-labile sample determined by DLS was $115.6 \pm 5.9 \text{ nm}$ that was slightly larger than the control at $102.9 \pm 2.5 \text{ nm}$ ($p < 0.05$). This trend is consistent in the TEM analysis (figure 4). The DLS analysis also generated a polydispersity index (PDI) of 0.26 ± 0.02 (control) and 0.20 ± 0.01 (mPEG-PLA-SS-Cur). TEM analysis revealed that the mean core size of mPEG-PLA-SS-Cur was $94.1 \pm 7.4 \text{ nm}$ in contrast to the mPEG-PLA-Cur control at $83.9 \pm 9.9 \text{ nm}$ ($p < 0.05$). As expected, the TEM size is smaller than the corresponding hydrodynamic (DLS) diameter for both samples. These sizes would help the conjugate micelles utilize the passive tissue targeting via enhanced permeability and retention effect upon *in vivo* administration [21, 22]. In addition, it is also feasible to finely tune the ratio of hydrophilic and hydrophobic block of the copolymer, as well as the whole molecular weight, to optimize the particle size and manipulate delivery efficiency.

The micelle stability was assessed using the CMC as an index (figure 5). The CMC determined via fluorescence methods was $6.7 \pm 0.4 \mu\text{g mL}^{-1}$ (redox-labile micelle) and $7.1 \pm 0.9 \mu\text{g mL}^{-1}$ (control), respectively. The corresponding molar concentration was $1.6 \pm 0.1 \mu\text{M}$ (mPEG-PLA-SS-Cur) and $1.7 \pm 0.2 \mu\text{M}$ (mPEG-PLA-Cur) using the M_n obtained by ^1H NMR. For both units, there was no significant difference between two samples ($p > 0.05$). It was previously reported that mPEG-PLA with similar M_n and block ratio showed a CMC value of $27.4 \pm 0.8 \mu\text{g mL}^{-1}$ [15]. Since the impelling force of micelle formation is the decrease of free energy in the aqueous medium, upon conjugate assembly, the hydrophobic block moves towards the micelle core and the hydrophilic mPEG block is exposed to the water forming a stabilization shell [23]. In the current study, the hydrophobic curcumin ($\log P = 3.2$) was linked to the hydrophobic PLA block, which would facilitate the conjugate self-assembly. This resulted in a dramatic CMC reduction for both conjugate micelles in comparison to mPEG-PLA micelles, and hence the significantly enhanced stability of conjugate micelles. Such a feature is beneficial to maintain the micelle integrity under *in vivo* situations, which is critical for an efficient delivery system [24].

A full ultraviolet (UV) scan showed that both conjugates exhibit a considerable peak shift compared to curcumin (data not shown). Hence it is not feasible to quantify the drug loading of conjugate samples using the typical UV/HPLC methods. As an alternative, the ^1H NMR analysis showed a drug loading of 8.2% (w/w) (mPEG-PLA-SS-Cur) and 5.8%

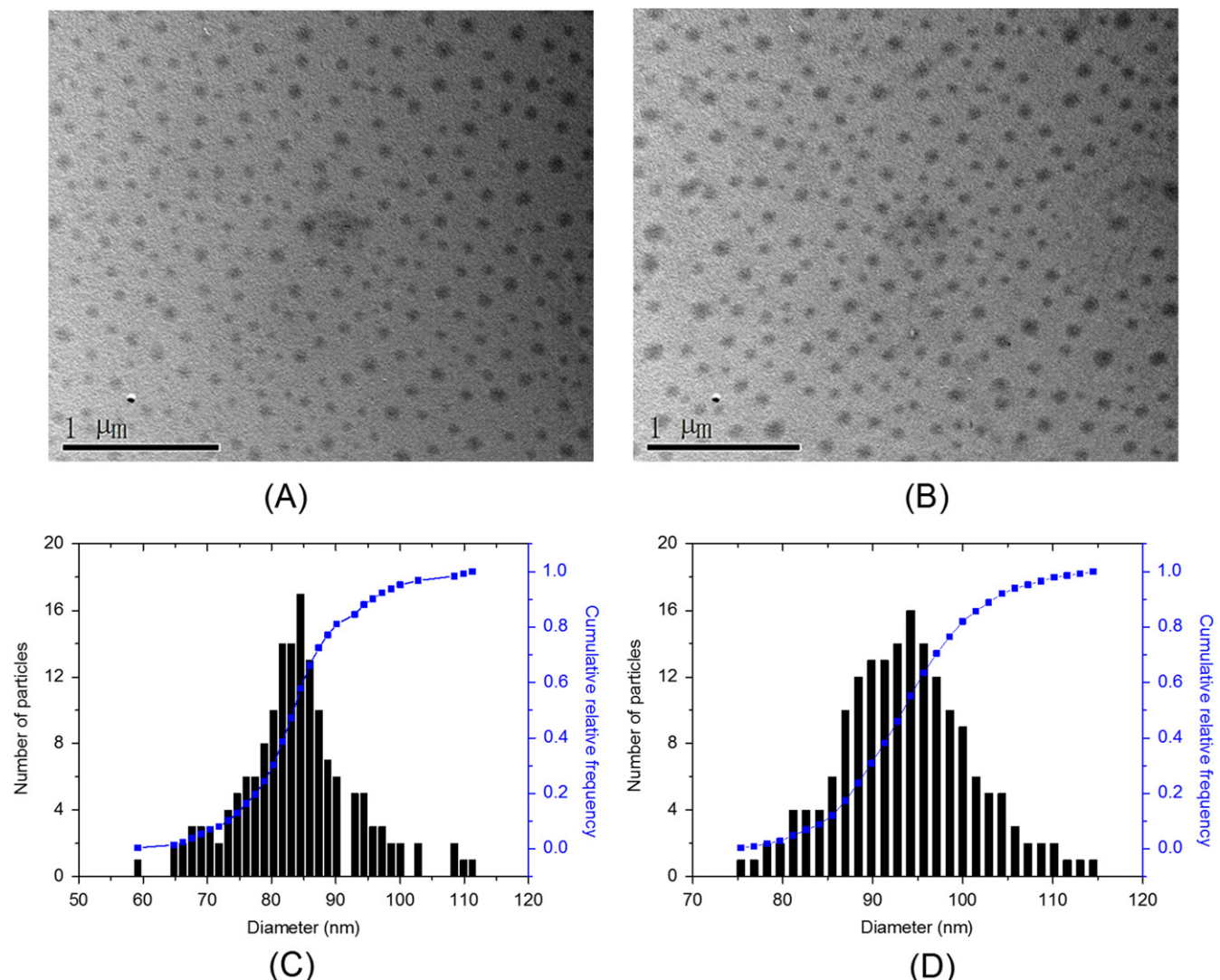


Figure 4. Transmission electron microscopy (TEM) analysis of ester bond-linked polymer-drug conjugate micelles mPEG-PLA-Cur (A), (C) and disulfide bond-linked conjugate mPEG-PLA-SS-Cur micelles (B), (D). The upper panels show the TEM images of conjugate micelles, and the lower panels show the number-based distribution of the core diameter of the corresponding micelles ($n=200$). Scale bar: 1 μm .

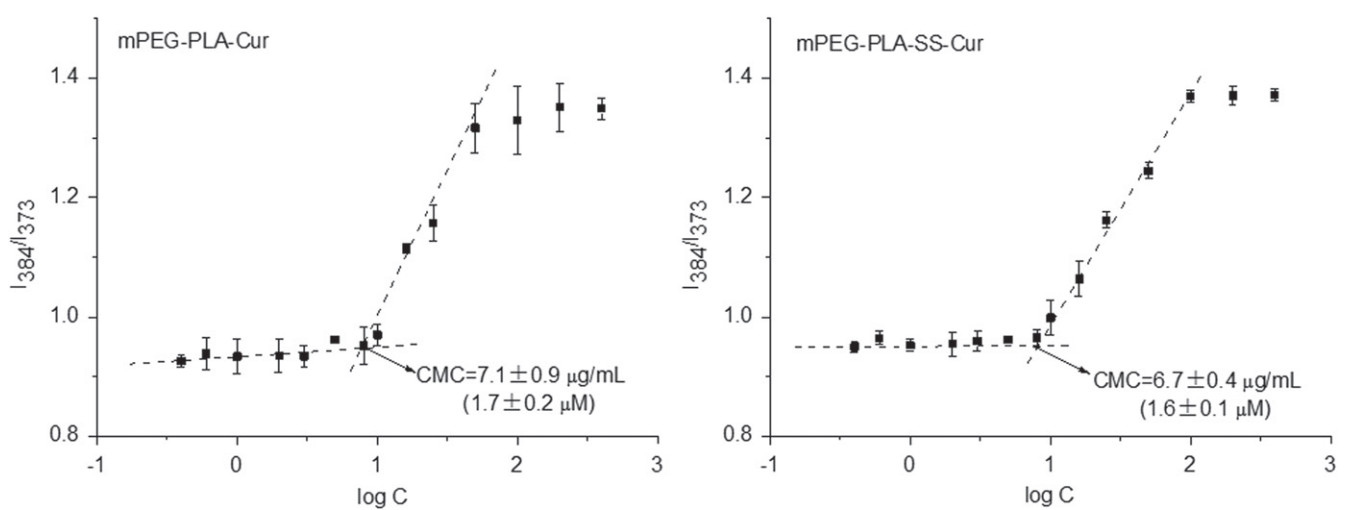


Figure 5. Critical micelle concentration (CMC) plot of two types of polymer-drug conjugates (mPEG-PLA-Cur and mPEG-PLA-SS-Cur). The CMC data were presented as mean \pm standard deviation at both weight and molar concentration of the conjugate ($n=3$).

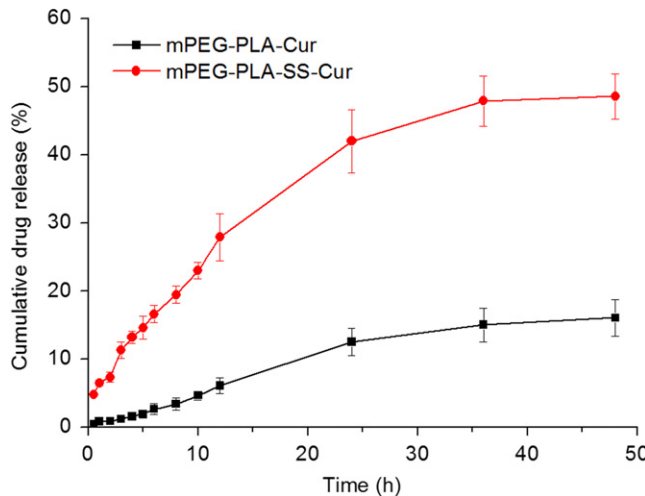


Figure 6. *In vitro* curcumin release profile from two types of polymeric conjugate micelles (mPEG-PLA-Cur and mPEG-PLA-SS-Cur) at 37 °C and pH 7.4 ($n=3$). The release study was carried out under sink conditions with 10 mM dithiothreitol to mimic the reduction environment inside the cells. The drug was linked to the polymer via ester (mPEG-PLA-Cur) and disulfide (mPEG-PLA-SS-Cur) bond, respectively.

(w/w) (mPEG-PLA-Cur). The drug release test was performed under sink conditions using a previously published method with minor modification [25]. The presence of DTT in the receiver fluid is to mimic the role of glutathione (GSH) in the cells. DTT usually broke down the disulfide bond more efficiently than GSH and had been widely used to test the redox-sensitive systems *in vitro* [26, 27]. The drug release rate and extent from disulfide-containing mPEG-PLA-SS-Cur conjugate micelles was much higher compared to the control (mPEG-PLA-Cur) (figure 6). At 48 h, only 16±4% of curcumin was released via hydrolysis from the mPEG-PLA-Cur control, whereas the drug amount released from redox-responsive conjugate (mPEG-PLA-SS-Cur) reached 16±4%. The thiol-disulfide exchange reaction by which DTT takes the action is considered faster than the enzymolysis process. This concurred well with previous work on redox-responsive and esterase-sensitive polymeric micelles [15, 28]. At the end of therelease experiment, the mass balance study showed a drug recovery of 84±4% (mPEG-PLA-SS-Cur) and 81±2% (control), respectively. The mass balance results also agreed well with a previous investigation using a similar testing system [19].

The dose-responsive cell viability gave an indication of the cytotoxicity profile of both conjugate micelles (figure 7). The IC₅₀ of mPEG-PLA-SS-Cur micelles was 18.5±1.4 ($\mu\text{g mL}^{-1}$), which corresponded to a molar concentration of 4.4±0.3 (μM). In contrast, the IC₅₀ of control micelles (mPEG-PLA-Cur micelles) was 41.0±2.4 ($\mu\text{g mL}^{-1}$) or 9.9±0.6 (μM). The IC₅₀ of free curcumin was 13.2±1.7 ($\mu\text{g mL}^{-1}$) or 35.9±4.6 (μM). The redox-sensitive conjugate micelles displayed significantly higher cytotoxicity than did the control micelles ($p<0.05$). This result correlated well with the drug release profile (figure 6). It was presumed that rapid drug release was vital to achieve a higher

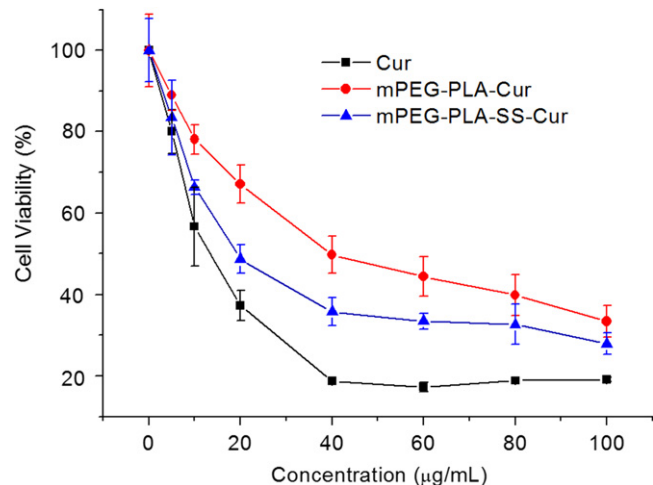


Figure 7. The dose-dependent cell viability of HeLa cells in response to free curcumin (Cur), mPEG-PLA-Cur micelle, and mPEG-PLA-SS-Cur micelle ($n \geq 4$). The sample concentration ranged from 0 to 100 $\mu\text{g mL}^{-1}$.

cytotoxicity, which was also observed in previous work that designed pH-responsive conjugate micelles [19]. Indeed, the cytotoxicity results agreed well with the drug release data.

The cellular internalization of the conjugate micelles as well as curcumin by HeLa cells were assessed by confocal microscopy (figure 8). Curcumin, its derivative, and polymer-curcumin all show inherent fluorescence [15, 19], and hence it is not necessary to label the conjugate micelles with additional fluorescent dyes. In addition, the presence of fluorescent labeling molecules might influence the nanoparticle properties [29]. Irrespective of the image acquisition time, the redox-labile mPEG-PLA-SS-Cur exhibited stronger green fluorescence than the control micelle. DAPI (blue fluorescence) was used to stain the nuclei of the HeLa cells. The co-localization images showed that both conjugate micelles mainly accumulated in the cytoplasmic compartment without substantial nuclear entry. Such a phenomenon was also seen in a previous report of curcumin-loaded nanoparticles [30]. However, for the curcumin control there was considerable amount of drug staining within the nuclei, which was also reported previously [15]. Nanoparticles are usually internalized via complicated mechanisms such as caveolae-mediated endocytosis, clathrin-mediated endocytosis, and macropinocytosis. Since there was no substantial difference between the redox-labile conjugate micelle and the control micelle in terms of physicochemical property e.g. size, surface charge, shape and rigidity, the cellular uptake efficiency of both samples via endocytosis was presumed similar. The higher fluorescence intensity of mPEG-PLA-SS-Cur compared with the control is most likely due to higher drug loading in the tested system. Assuming the same amount of micelles were internalized, the redox-sensitive one would have carried more curcumin and hence displayed higher fluorescence. Compared to the free curcumin (control) that was distributed both in the cytoplasm and nucleus, the conjugate micelle-loaded curcumin primarily resided in the

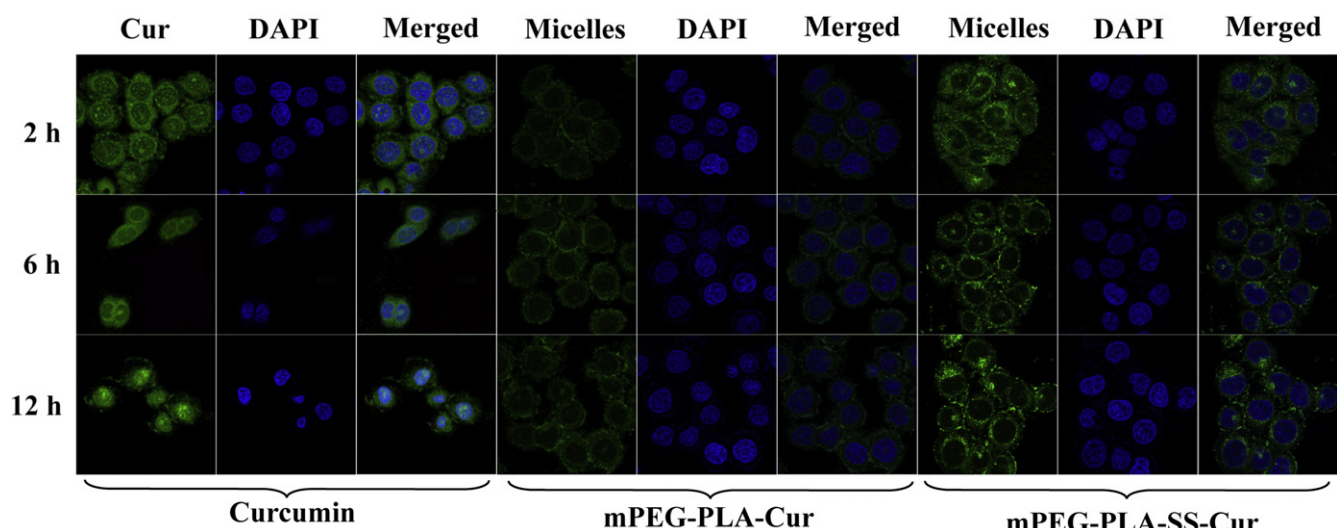


Figure 8. Intracellular curcumin delivery: free curcumin (Cur, column 1–3), mPEG-PLA-Cur micelle (column 4–6), and mPEG-PLA-SS-Cur micelle (column 7–9) in HeLa cells at different time points post incubation. Images were taken via confocal laser scanning microscopy. The green and blue color signifies the micelles/drug and cell nuclei, while the merged pictures were given to show the location of micelles/drug inside the cells. Scale bar: 10 µm.

cytoplasmic compartment. Despite the different cellular uptake mechanism, this phenomenon might be partly due to the inefficiency of endosomal escape for conjugate micelles. Upon endocytosis, the micelles have to get out of the acidic endosomes/lysosomes prior to distribution in the subcellular organelles [31]. The lack of such capability would delay or affect the curcumin's nuclear entry, as observed in the current study as well as in previous work [15, 32].

4. Conclusions

Redox-responsive polymer-curcumin conjugate micelles are reported to address the challenge of premature versus on-demand drug release. Such a strategy could extend to other active agents and amphiphilic polymers with reactive conjugation sites (e.g. -NH₂, -COOH, -OH). Usually a disulphide-containing linker is required to endow the nanoparticle with redox sensitivity. However, certain drugs might not have such active sites for conjugation and this strategy might not be applicable for all drugs. For some hydrophilic drugs, their presence might deteriorate the stability of the conjugate micelles. In addition, other factors such as endosomal escape are often considered as one of the bottlenecks of redox-responsive triggered-release of nanoscale drug delivery systems for efficient intracellular delivery of therapeutic payloads. These factors merit further investigation in other therapeutic settings in order to ultimately translate these strategies into clinical practice.

Acknowledgments

This work was supported by the National Natural Science Foundation of China (2134068), National Basic Research Program of China (2015CB856500), Tianjin Research

Program of Application Foundation and Advanced Technology (13JCQNJC13300, 14JCZDJC38400), and the Open Fund of State Key Laboratory of Medicinal Chemical Biology, Nankai University (20130557). This work was supported in part by grants from the Israeli Center of Research Excellence (I-CORE), Gene Regulation in Complex Human Disease, Center No 41/11; FTA: Nanomedicine for Personalized Therapeutics, and by The Leona M. and Harry B. Helmsley Nanotechnology Research Fund awarded to D.P.

Conflicts of interest

The authors of this article have no conflicts of interest to declare.

References

- [1] Yoo H S, Lee K H, Oh J E and Park T G 2000 *In vitro* and *in vivo* anti-tumor activities of nanoparticles based on doxorubicin-PLGA conjugates *J. Controlled Release* **68** 419–31
- [2] Peer D, Karp J M, Hong S, Farokhzad O C, Margalit R and Langer R 2007 Nanocarriers as an emerging platform for cancer therapy *Nat. Nanotechnol.* **2** 751–60
- [3] Paraskar A, Soni S, Roy B, Papa A L and Sengupta S 2012 Rationally designed oxaliplatin-nanoparticle for enhanced antitumor efficacy *Nanotechnology* **23** 075103
- [4] Bachar G, Cohen K, Hod R, Feinmesser R, Mizrahi A, Shpitzer T, Katz O and Peer D 2011 Hyaluronan-grafted particle clusters loaded with mitomycin C as selective nanovectors for primary head and neck cancers *Biomaterials* **32** 4840–8
- [5] Parhi P, Mohanty C and Sahoo S K 2012 Nanotechnology-based combinational drug delivery: an emerging approach for cancer therapy *Drug Discovery Today* **17** 1044–52
- [6] Zhang Q, Zhu J, Song L, Zhang J, Kong D, Zhao Y and Wang Z 2013 Engineering magnetic-molecular sequential targeting nanoparticles for anti-cancer therapy *J. Mater. Chem. B* **1** 6402–10

- [7] He Q and Shi J 2014 MSN anti-cancer nanomedicines: chemotherapy enhancement, overcoming of drug resistance, and metastasis inhibition *Adv. Mater.* **26** 391–411
- [8] Ganoth A, Merimi K C and Peer D 2014 Dry powder inhalers in COPD, lung inflammation and pulmonary infections *Expert Opin. Drug Deliv.* **12** 1–16
- [9] Wang Z, Chen C, Liu R, Fan A, Kong D and Zhao Y 2014 Two birds with one stone: dendrimer surface engineering enables tunable periphery hydrophobicity and rapid endosomal escape *Chem. Commun.* **50** 14025–8
- [10] Drinberg V, Bitcover R, Rajchenbach W and Peer D 2014 Modulating cancer multidrug resistance by sertraline in combination with a nanomedicine *Cancer Lett.* **354** 290–8
- [11] Zhao J, Vyková J, Abdelsalam M, Recio-Boiles A, Huang Q, Qiao Y, Singhana B, Wallace M, Avritscher R and Melancon M P 2014 Stem cell-mediated delivery of SPIO-loaded gold nanoparticles for the theranosis of liver injury and hepatocellular carcinoma *Nanotechnology* **25** 405101
- [12] Cohen K, Emmanuel R, Kislin-Finfer E, Shabat D and Peer D 2014 Modulation of drug resistance in ovarian adenocarcinoma using chemotherapy entrapped in hyaluronan-grafted nanoparticle clusters *ACS Nano* **8** 2183–95
- [13] Miller T, Breyer S, van Colen G, Mier W, Haberkorn U, Geissler S, Voss S, Weigandt M and Goepfert A 2013 Premature drug release of polymeric micelles and its effects on tumor targeting *Int. J. Pharm.* **445** 117–24
- [14] Zhao Y, Moddaresi M, Jones S A and Brown M B 2009 A dynamic topical hydrofluoroalkane foam to induce nanoparticle modification and drug release *in situ* *Eur. J. Pharm. Biopharm.* **72** 521–8
- [15] Yang R, Zhang S, Kong D, Gao X, Zhao Y and Wang Z 2012 Biodegradable polymer-curcumin conjugate micelles enhance the loading and delivery of low-potency curcumin *Pharm. Res.* **29** 3512–25
- [16] Li Y, Xiao K, Zhu W, Deng W and Lam K S 2014 Stimuli-responsive cross-linked micelles for on-demand drug delivery against cancers *Adv. Drug Delivery Rev.* **66** 58–73
- [17] Fleige E, Quadir M A and Haag R 2012 Stimuli-responsive polymeric nanocarriers for the controlled transport of active compounds: concepts and applications *Adv. Drug Delivery Rev.* **64** 866–84
- [18] Sun H, Meng F, Cheng R, Deng C and Zhong Z 2013 Reduction-sensitive degradable micellar nanoparticles as smart and intuitive delivery systems for cancer chemotherapy *Expert Opin. Drug Delivery* **10** 1109–22
- [19] Wang Z, Chen C, Zhang Q, Gao M, Zhang J, Kong D and Zhao Y 2015 Tuning the architecture of polymeric conjugate to mediate intracellular delivery of pleiotropic curcumin *Eur. J. Pharm. Biopharm.* at press doi:10.1016/j.ejpb.2014.11.002
- [20] Izunobi J U and Higginbotham C L 2011 Polymer molecular weight analysis by ^1H NMR spectroscopy *J. Chem. Educ.* **88** 1098–104
- [21] Maeda H 2012 Macromolecular therapeutics in cancer treatment: the EPR effect and beyond *J. Controlled Release* **164** 138–44
- [22] Bogart L K, Pourroy G, Murphy C J, Puntes V, Pellegrino T, Rosenblum D, Peer D and Lévy R 2014 Nanoparticles for imaging, sensing, and therapeutic intervention *ACS Nano* **8** 3107–22
- [23] Torchilin V 2007 Micellar nanocarriers: pharmaceutical perspectives *Pharm. Res.* **24** 1–16
- [24] Owen S C, Chan D P Y and Shoichet M S 2012 Polymeric micelle stability *Nano Today* **7** 53–65
- [25] Fu Y, Gao X, Wan Y, Zhang J, Kong D, Wang Z and Zhao Y 2014 Dendritic nanoconjugate containing optimum folic acid for targeted intracellular curcumin delivery *RSC Adv.* **4** 46020–3
- [26] Liu J, Huang W, Pang Y, Huang P, Zhu X, Zhou Y and Yan D 2011 Molecular self-assembly of a homopolymer: an alternative to fabricate drug-delivery platforms for cancer therapy *Angew. Chem. Int. Ed.* **50** 9162–6
- [27] Remant B K, Chandrasekaran V, Cheng B, Chen H, Peña M M, Zhang J, Montgomery J and Xu P 2014 Redox potential ultrasensitive nanoparticle for the targeted delivery of camptothecin to HER2-positive cancer cells *Mol. Pharm.* **11** 1897–905
- [28] Zhong Y, Yang W, Sun H, Cheng R, Meng F, Deng C and Zhong Z 2013 Ligand-directed reduction-sensitive shell-sheddable biodegradable micelles actively deliver doxorubicin into the nuclei of target cancer cells *Biomacromolecules* **14** 3723–30
- [29] Saptarshi S R, Duschl A and Lopata A L 2013 Interaction of nanoparticles with proteins: relation to bio-reactivity of the nanoparticle *J. Nanobiotechnol.* **11** 26
- [30] Tang H, Murphy C J, Zhang B, Shen Y, Van Kirk E A, Murdoch W J and Radosz M 2010 Curcumin polymers as anticancer conjugates *Biomaterials* **31** 7139–49
- [31] Cai T, Lei Q, Yang B, Jia H, Cheng H, Liu L, Zeng X, Feng J, Zhuo R and Zhang X 2014 Utilization of H-bond interaction of nucleobase Uralic with antitumor methotrexate to design drug carrier with ultrahigh loading efficiency and pH-responsive drug release *Regen. Biomater.* **1** 27–35
- [32] Kunwar A, Barik A, Mishra B, Rathinasamy K, Pandey R and Priyadarshini K I 2008 Quantitative cellular uptake, localization and cytotoxicity of curcumin in normal and tumor cells *Biochim. Biophys. Acta* **178** 673–9